*Accelerated Publications*

# The Werner Syndrome Helicase/Exonuclease (WRN) Disrupts and Degrades D-Loops in Vitro†

David K. Orren,* Shaji Theodore, and Amrita Machwe

*Graduate Center for Toxicology, University of Kentucky, Lexington, Kentucky 40536*

*Received August 21, 2002; Revised Manuscript Received September 25, 2002*

ABSTRACT: The loss of function of WRN, a DNA helicase and exonuclease, causes the premature aging disease Werner syndrome. A hallmark feature of cells lacking WRN is genomic instability typified by elevated illegitimate recombination events and accelerated loss of telomeric sequences. In this study, the activities of WRN were examined on a displacement loop (D-loop) DNA substrate that mimics an intermediate formed during the strand invasion step of many recombinational processes. Our results indicate that this model substrate is specifically bound by WRN and efficiently disrupted by its helicase activity. In addition, the 3′ end of the inserted strand of this D-loop structure is readily attacked by the 3′→5′ exonuclease function of WRN. These results indicate that D-loop structures are favored sites for WRN action. Thus, WRN may participate in DNA metabolic processes that utilize these structures, such as recombination and telomere maintenance pathways.

Werner syndrome (WS)[1] is an autosomal recessive disease characterized by early onset and increased frequency of age-related maladies including atherosclerosis, cataracts, and cancer (reviewed in refs *1* and *2*). Cells derived from WS patients display genomic instability typified by increased deletions, insertions, and translocations (*3*, *4*) as well as accelerated shortening of telomeric sequences (*5*, *6*). Amazingly, the accelerated aging phenotype of WS is caused by defects in a single gene, known as *WRN*, that encodes a protein with homology to the RecQ family of nucleic acid helicases (*7*). In general, RecQ helicase deficiencies result in increased illegitimate recombination events, suggesting roles for these proteins in normal recombination or perhaps anti-recombinogenic pathways (*8*).

Purified WRN protein has been shown to have DNA-dependent ATPase and unwinding (3′ → 5′ directionality) activities consistent with its RecQ classification (*9*, *10*). WRN helicase acts on a variety of DNA structures but seems to be directed preferentially to junctions between single- and double-stranded DNA (*11*). However, WRN also harbors a 3′→5′ exonuclease activity unique among the five human RecQ members (*12*, *13*). Interestingly, all of the mutations described in WS patients truncate WRN prior to its C-terminal nuclear localization signal and likely result in the inability of mutant proteins to even enter the nucleus (*1*). Thus, the WS syndrome phenotype may be due to loss of both helicase and exonuclease activities.

An early step in many recombination pathways is invasion of single-stranded DNA (frequently containing a 3′ end) into a homologous duplex to form a displacement loop (D-loop) structure (*14*, *15*). Within the D-loop structure, the junctions between single- and double-stranded DNA and the available 3′ end are potential sites for WRN helicase and exonuclease activities, respectively. To address this possibility, we examined the DNA binding and catalytic activities of WRN on a specially constructed D-loop substrate. Importantly, D-loop structures are specifically and stably bound with high affinity by WRN and efficiently disrupted by WRN helicase activity. Moreover, the invading strand in the D-loop is readily attacked and degraded from its 3′ end by the exonuclease activity of WRN. Our results are consistent with a role for WRN in processing of D-loop intermediates that arise during DNA metabolism.

## EXPERIMENTAL PROCEDURES

*WRN Purification.* Both wild-type and mutant WRN proteins used in this study were overproduced and purified as previously described (*16*). The WRN-E84A mutant has a glutamate to alanine mutation at amino acid 84 in the exonuclease domain. This mutation abolishes exonuclease activity, but helicase activity is retained (*17*).

*DNA Substrates*. Oligonucleotides were purchased from Integrated DNA Technologies (Coralville, IA) and Operon (Alameda, CA). In 5′ to 3′ orientation, oligonucleotide sequences were FD80 (AGCTCCTAGGGTTACAAGCT-

† This work was supported in part by funds provided by Grant NS-008900 from the Ellison Medical Foundation and Grant 85-001-13-IRG from the American Cancer Society (to D.K.O.).

* To whom correspondence should be addressed. Telephone: 859-323-3612. Fax: 859-323-1059. E-mail: dkorre2@pop.uky.edu.

[1] Abbreviations: WS, Werner syndrome; nt, nucleotides; PAGE, polyacrylamide gel electrophoresis; BPB, bromphenol blue; XC, xylene cyanol; EMSA, electrophoretic mobility shift assay; ATPγS, adenosine 5′-*O*-(3-thiotriphosphate); DNase I, bovine pancreatic deoxyribonuclease I; bp, base pairs.

10.1021/bi0266986 CCC: $22.00 
Published on Web 10/22/2002

TCACTAGGGTTGTCCTTAGGGTTAGGGTTAGGGTTA-CCTACACATGTAGGGTTGATCAGC), DL80-D (AGC-TCCTAGGGTTACAAGCTTCACTAGGGTTGTCCAGT-CACAGTCAGAGTCACA GTCCTACACATGTAGGGT-TGATCAGC), DL80-P (GCTGATCAACCCTACATGTG-TAGGTAACCCTAACCCTAACCCTAAGGACAACCCTA-GTGAAGCTTGTAACCCTAGGAGCT), INV5′A15 (AAA-AAAAAAAAAAAAATTAGGGTTAGGGTTAGGGTTA), INV (TTAGGGTTAGGGTTAGGGTTA), and INV3′A15 (TTAGGGTTAGGGTTAGGGTTAAAAAAAAAAA AAA-AA). For exonuclease assays, some substrates were constructed with DL80-P and DL80-D oligomers containing $PO_4$ groups at the 3′ ends. Phosphorothioate linkage was introduced between the 5′ end and 5′ penultimate nucleotides of all the above oligonucleotides to prevent the 5′→3′ nuclease activity of a minor contaminant present in some WRN preparations. Where indicated, oligonucleotides were radiolabeled at their 5′ terminus with [$\gamma$-$^{32}$P]ATP (3000 Ci/mmol), and T4 polynucleotide kinase, 3′-phosphatase free (Roche Molecular Biochemicals, Indianapolis, IN), and unincorporated radionucleotides were removed using standard methods. A 2-fold excess of unlabeled FD80 or DL80-D was annealed to labeled DL80-P to form fully duplex or bubble substrates, respectively, by heating at 90 °C for 5 min and slow cooling to 25 °C. Duplex and bubble substrates were separated from excess single-stranded oligomers by native polyacrylamide (12%) gel electrophoresis (PAGE), recovered using a gel extraction kit (Qiagen, Valencia, CA), and stored in 10 mM Tris-HCl, pH 8.0 at 4 °C. To form D-loop substrates, equimolar amounts of oligonucleotide INV5′A15, INV, or INV3′A15 (unlabeled or labeled as described above) were annealed to the bubble substrate by heating the mixture to 70 °C for 15 min and slowly cooling to 25 °C. Correct annealing of the substrates was confirmed by individual digestions with the restriction enzymes *Hin*dIII, *Bfa*I, and *Nsp*I followed by inspection of DNA products after PAGE.

*DNA Unwinding Assay.* For unwinding assays, the bubble substrate constructed with labeled DL80-P oligomer was used with or without an annealed, labeled INV5′A15, INV, or INV3′A15 oligomer. Bubble and D-loop substrates (0.25−1.0 fmol) were incubated with WRN-E84A (0.38−12 fmol) in WRN buffer [40 mM Tris-HCl (pH 8.0), 4 mM $MgCl_2$, 0.1 mg/mL bovine serum albumin, and 5 mM dithiothreitol] for 15 min at 37 °C in the presence of ATP (1 mM). Reactions were stopped with one-sixth volume of helicase stop dye [30% glycerol, 50 mM EDTA, 0.9% SDS, 0.25% bromphenol blue (BPB), and 0.25% xylene cyanol (XC)]. The DNA products were then separated by 8% PAGE. Gels were vacuum-dried and analyzed using a Storm 860 Phosphorimager and ImageQuant software (Molecular Dynamics, Sunnyvale, CA). Quantitation of D-loop unwinding was determined by comparing amounts of labeled INV5′A15 or INV oligomer displaced with total amounts of the same oligomer present in the untreated D-loop.

*Exonuclease Assay.* For the exonuclease assay, the DL80-P and DL80-D oligomers had 3′-$PO_4$ modifications, and both DL80-P and INV5′A15 (36 nt) oligomers were labeled. D-loop substrates (1.2 fmol) were incubated for 1 h at 37 °C with wild-type WRN (1−8 fmol) or WRN-E84A (5−45 fmol) in WRN buffer without ATP. Reactions were stopped with equal volumes of formamide dyes (95% formamide, 20 mM EDTA, 0.1% BPB, and 0.1% XC). DNA products were heat-denatured, run on denaturing 14% PAGE, and analyzed as above.

*Electrophoretic Mobility Shift Assay (EMSA).* DNA substrates for EMSA were constructed using labeled DL80-P with unlabeled FD80 or DL80-D and annealing unlabeled INV5′A15 when needed to form the D-loop substrate. Fully duplex, bubble, and D-loop substrates (0.6 fmol) were incubated 30 min at 4 °C with wild-type WRN (9−90 fmol) in WRN buffer plus 0.1% Nonidet P-40 and ATP$\gamma$S (1 mM). After addition of one-sixth volume of native dye (30% glycerol, 0.25% BPB, and 0.25% XC), DNA and DNA−protein complexes were separated at 4 °C by 4% PAGE and analyzed as above. Binding was quantitated by comparing the amount of unbound DNA with the total DNA in the reaction (% $DNA_{bound} = [(DNA_{total} - DNA_{unbound})/DNA_{total}] \times 100$).

*DNase I Footprinting.* Bubble and D-loop substrates for DNase I footprinting analysis were as described for the exonuclease assay, except the D-loop substrate was made with unlabeled INV5′A15 oligomer. DNA substrates (2.4 fmol) were incubated with wild-type WRN (3−36 fmol) in WRN buffer plus ATP$\gamma$S (1 mM) for 30 min at 4 °C, followed by 10 min at 4 °C with DNase I (1 unit). Reactions were stopped and treated as for the exonuclease assay. Nucleotide size markers were created as described previously (*17*). The binding affinity of WRN to bubble and D-loop substrates was compared by measuring (via phosphorimaging analysis) the disappearance of specific bands from the DNase I digestion pattern with increasing WRN concentration.

## RESULTS

An early step in many recombination pathways is invasion of a single-stranded DNA with a 3′ end into a homologous duplex to form a D-loop structure (*14*, *15*). To investigate a potential role for WRN in metabolism of these structures, a model substrate was constructed by first annealing partially complementary 80 nt oligomers to form a duplex with a 21 nt bubble and then annealing a third (invading) strand to form a D-loop at the site of the bubble (Figure 1A). Formation of the proposed D-loop structure was confirmed by its retarded migration on nondenaturing gels and the complete cleavage of the 35 and 24 bp arms by restriction endonucleases (Figure 1B).

First, WRN binding to the D-loop substrate was examined by EMSA and DNase I protection assays. By EMSA, WRN binds to the D-loop substrate with higher affinity (more than 2-fold at limiting WRN concentration) than to the comparable bubble substrate without the inserted strand (Figure 2A,B). These DNA−protein complexes contain WRN, as they are supershifted by WRN-specific antibodies (data not shown). Using this EMSA method, WRN does not detectably bind to a fully duplex substrate (Figure 2A) or to substrates containing simple forks, 3′ or 5′ single-stranded overhangs, and only single-stranded DNA (data not shown). These data indicate that WRN binds strongly and specifically to the bubble and D-loop structures with no detectable affinity for sequences within the substrate. DNase I protection assays were used to pinpoint the region of the substrate that was bound by WRN. WRN protected part of one strand (DL80-P) that formed the duplex part of the D-loop structure and elicited multiple DNase I hypersensitive sites on the 35 bp

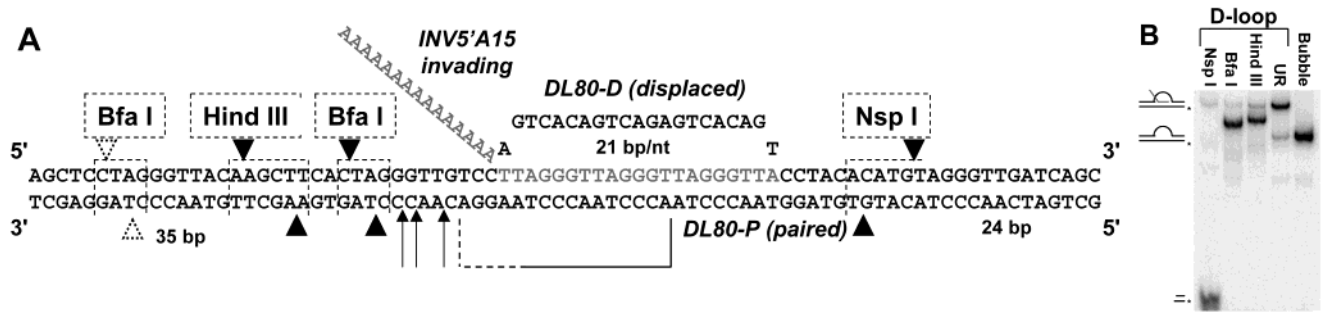


FIGURE 1: D-loop substrate structure. (A) Sequence and structure of the D-loop substrate. The partially complementary DL80-P (paired) and DL80-D (displaced) oligomer sequences are in bold and the INV5′A15 (invading) oligomer is in lightly shaded type, with lengths of the duplex arms and D-loop region noted. Selected restriction enzyme recognition sequences and their incision sites are denoted by dashed boxes and arrowheads [solid for those sites utilized in (B)], respectively. As evidenced by DNase I footprinting (see Figure 2C), the region of WRN binding to the DL80-P strand of this substrate is indicated by right angle brackets (solid and dashed lines denoting observed and putative areas of binding, respectively), and the associated DNase I hypersensitive sites are designated by arrows. (B) D-loop substrate structure analysis. After complete annealing, the D-loop substrate was digested by *Nsp*I, *Bfa*I, or *Hin*dIII, and products were separated by 8% PAGE along with unrestricted (UR) D-loop and bubble substrates. The positions of the D-loop, the bubble substrate, and the *Nsp*I fragment are denoted at the left, with positions of radiolabels indicated by asterisks.

arm 4−8 nt from the D-loop junction (Figure 2C). The WRN footprint and associated DNase I hypersensitive sites on the DL80-P strand of the D-loop substrate are mapped on the substrate diagram (see Figure 1A). When compared to the bubble substrate, the protected area on the D-loop substrate is smaller (10−20 nt) and shifted toward the 35 bp arm (Figure 2C). These data suggest that WRN binds, at least in part, to the point where the invading strand exits the D-loop structure, although we cannot rule out the possibility that WRN might also bind to the displaced (DL80-D) strand. Over a limiting range of WRN concentration (6−18 fmol), a higher percentage of D-loop than bubble substrate was bound by WRN, as assessed by disappearance of specific bands (indicated by asterisks) from the DNase I digestion pattern. Thus, both EMSA and footprinting assays suggest that D-loop structures are preferred even over bubble structures previously shown to be high-affinity substrates for WRN binding (*17*).

WRN has both DNA unwinding and 3′→5′ exonuclease activities; either (or both) could potentially disrupt D-loop structures. To specifically examine unwinding, assays were carried out with WRN-E84A mutant protein that lacks exonuclease but retains helicase activity (*17*). WRN-E84A was able to efficiently displace the invading strand of our substrate, converting the D-loop into a bubble (Figure 3A) in a reaction requiring ATP hydrolysis. The bubble structure was not unwound here, although much higher WRN concentrations (>60 fmol) can unwind these structures (*17*). Since WRN does bind single-stranded DNA (*16*), the 5′ single-stranded flap of the invading strand could be mediating unwinding. To address this possibility, another D-loop substrate was formed with the invading strand not having a 5′ flap, i.e, in which all 21 nt are paired with the DL80-P strand. WRN-E84A disrupted this substrate without the 5′ flap at least as well as the original D-loop substrate (Figure 3B,C), indicating that a 5′ flap on the invading strand plays no part in WRN-mediated disruption of D-loops. Another D-loop substrate with a 3′ single-stranded flap on the inserted strand was similarly disrupted (data not shown). Significant levels of unwinding occur at WRN concentrations that are nearly equimolar to the DNA substrate, attesting to the extreme efficiency of this reaction. These results indicate that the D-loop structure itself mediates the heightened substrate binding and displacement of the invading strand by WRN helicase.

The invading strand of D-loop structures may have a 3′ end that could be a putative target for the 3′→5′ exonuclease activity of WRN. Likewise, the inserted strand of our D-loop substrate has a 3′ end in a comparable orientation. However, unlike physiological D-loop structures, our model substrate has two additional 3′ ends on each duplex arm (see Figure 1A) that might be attacked by WRN exonuclease. Indeed, the blunt ends of bubble substrates (without an inserted strand) are efficiently digested by WRN exonuclease (*17*, *18*). To avoid digestion at these sites, substrate was assembled with both 80-mers modified with $PO_4$ at the 3′ end, while the invading, radiolabeled 36-mer contained the normal 3′-OH group. Importantly, DNA strands ending in 3′-$PO_4$ groups are highly resistant to WRN exonuclease activity.[2] Thus, this substrate can be used to examine WRN exonuclease activity specifically on the 3′ end of the invading strand. Exonuclease assays were carried out in the absence of ATP to prevent WRN helicase activity. Wild-type WRN did not detectably degrade the labeled DL80-P strand (80 nt) (Figure 4), confirming that its 3′-$PO_4$ end prevents exonuclease attack. In sharp contrast, the invading strand (36 nt) was digested from its 3′ end in a stepwise fashion (Figure 4, left). This activity is inherent to WRN, as WRN-E84A exonuclease mutant does not degrade this substrate (Figure 4, right). Thus, in the context of a D-loop, the 3′ end of the invading strand can be efficiently recognized and degraded by WRN exonuclease. Notably, both helicase and exonuclease activities are manifested on this D-loop substrate over roughly the same range of WRN concentration (compare Figures 3 and 4), suggesting that the binding affinity of WRN may underlie the heightened efficiency of each activity.

## DISCUSSION

The genomic instability phenotypes of WS and other RecQ helicase-deficient conditions are suggestive of defective recombination or anti-recombination pathways (*8*). A potential role for WRN in such pathways was assessed by examining its DNA binding, unwinding, and exonuclease

[2] A. Machwe and D. K. Orren, unpublished experiments.

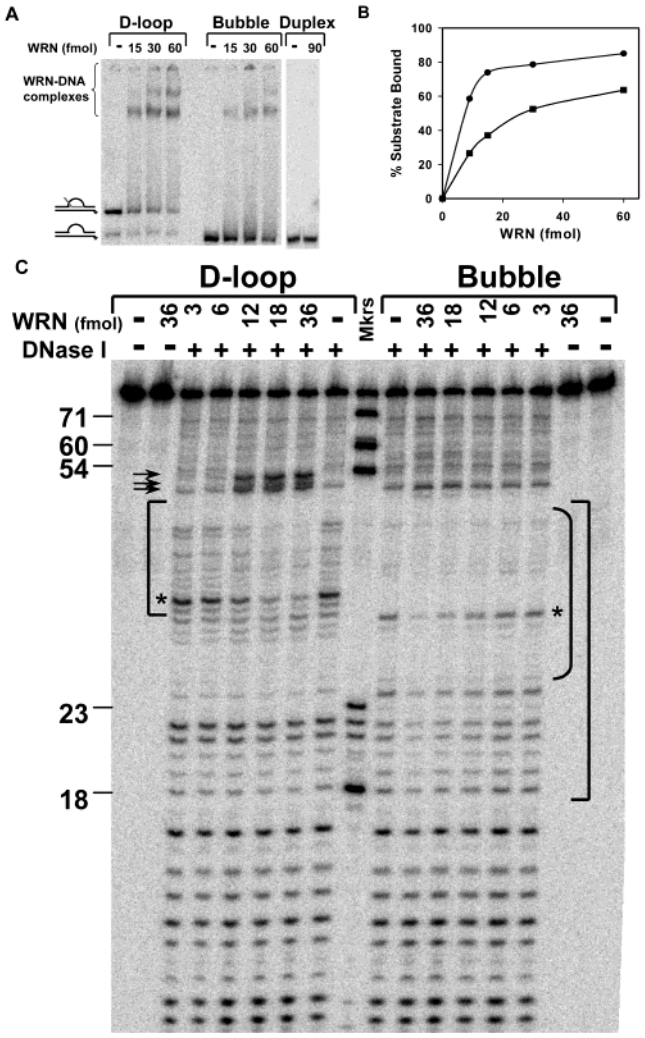


FIGURE 2: High-affinity WRN binding to the D-loop substrate. (A) DNA and DNA−protein complexes of wild-type WRN (15−90 fmol) with the D-loop, bubble, or duplex substrate were prepared and analyzed by EMSA as described in Experimental Procedures. The positions of WRN−DNA complexes and bubble and D-loop substrates are denoted. (B) Graphic representation of WRN binding to D-loop (●) and bubble (■) substrates, generated by EMSA [as visualized in (A)]. The amount of DNA substrate bound was determined from disappearance of the free DNA band. Data points are the mean of two independent experiments, except for values at 9 fmol of WRN. (C) Wild-type WRN (3−36 fmol) binding to D-loop (left) and bubble (right) substrates (both labeled on the DL80-P "paired" oligomer) analyzed by DNase I footprinting as described in Experimental Procedures. The lengths and positions of nucleotide markers are noted, as are the bounds of bubble and D-loop regions (curved bracket) and WRN "footprints" (right-angle brackets). Arrows mark DNase I hypersensitive sites caused by WRN binding to the D-loop substrate. Asterisks denote bands used to assess the relative binding of WRN to D-loop and bubble substrates.

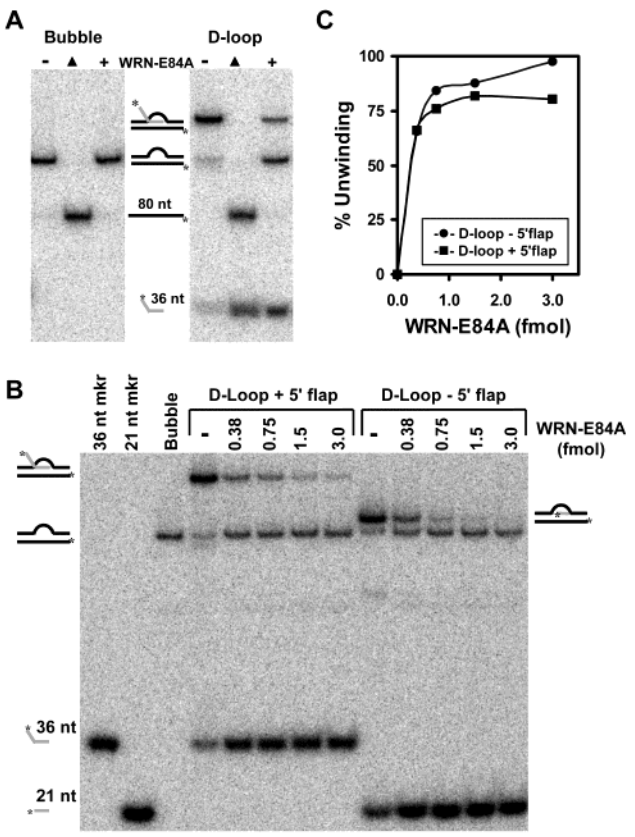


FIGURE 3: WRN-catalyzed unwinding of the D-loop substrate. (A) Reactions containing the bubble (labeled on the DL80-P oligomer) or D-loop (labeled on DL80-P and INV5′A15 oligomers) substrate (1 fmol) with or without exonuclease-deficient WRN-E84A (12 fmol) were analyzed for unwinding as described in Experimental Procedures. The positions of the D-loop, the bubble substrate, and DL80-P (80 nt) and INV5′A15 (36 nt) oligomers are denoted. (▲) substrates denatured by heating. (B) D-loop substrates (0.25 fmol) were constructed using labeled DL80-P with either labeled INV5′A15 (D-loop + 5′ flap) or labeled INV (D-loop − 5′ flap) oligomer and then subjected to the unwinding assay using WRN-E84A (0.38−3 fmol) as described in Experimental Procedures. The positions of the D-loop containing a 5′ flap, bubble substrate, and INV5′A15 (36 nt) and G21 (21 nt) oligomers are denoted at the left, with the D-loop without the 5′ flap noted at the right. (C) Quantitation of data presented in (B), comparing the amount of unwinding of the D-loop with (■) and without a 5′ flap (●).

activities on a D-loop substrate that approximates the structure formed during the strand invasion step of many recombination pathways. Our results indicate that WRN binds with high affinity to this substrate specifically in the region of the D-loop. This level of binding appears to be conferred by the structure of the D-loop, as WRN has lower affinity for bubble substrate without the inserted strand and no detectable affinity for a fully duplex DNA. The manner in which WRN binds to the D-loop substrate is markedly different than WRN binding to the same substrate without the inserted strand. When compared with the footprint of WRN on the bubble substrate, the D-loop footprint is more compact, with strong DNase I hypersensitive sites on the 35 bp duplex arm just 3′ to the D-loop structure on the DL80-P strand. The position of the footprint indicates that WRN binds (at least in part) near the junction where the invading strand exits the duplex. Both WRN helicase and exonuclease acted very efficiently on the D-loop substrate. The helicase activity of WRN easily dislodged the invading strand from the rest of the substrate, regardless of whether it contained a single-stranded flap 5′ or 3′ to the region of insertion. The efficient disruption of our D-loop substrate indicates that WRN translocation along single-stranded DNA 3′ to the duplex to be unwound is not required, consistent with a recent report (*11*) that WRN helicase may be targeted directly to junctions between single- and double-stranded DNA. However, stable binding to simple forked structures (as determined by EMSA) has not been demonstrated without the use of protein−DNA cross-linking agents, suggesting that D-loop structures form

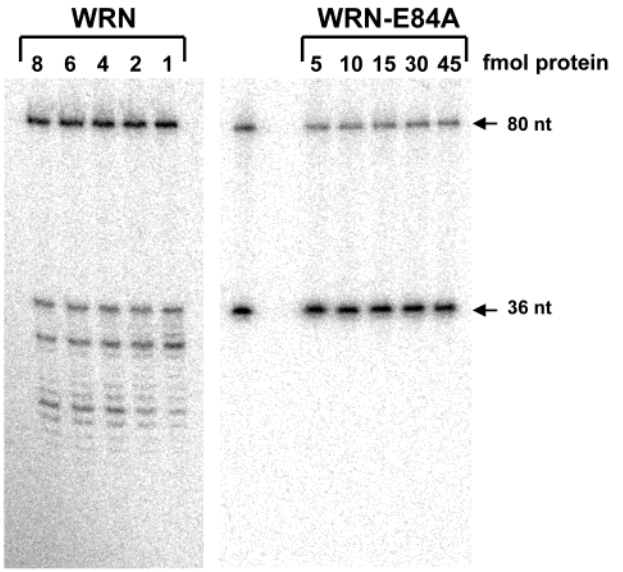


FIGURE 4: WRN exonuclease activity on the D-loop substrate. The D-loop substrate was constructed by annealing labeled INV5′A15 (containing the standard 3′-OH group) into the bubble substrate constructed from DL80-D and labeled DL80-P, both containing 3′-$PO_4$ ends. This substrate was incubated with either wild-type WRN (left, 1−8 fmol) or WRN-E84A (right, 5−45 fmol) in the absence of ATP to prevent unwinding, and DNA products were analyzed as described in Experimental Procedures. The positions of undigested DL80-P (80 nt) and INV5′A15 (36 nt) oligomers are denoted.

a much more stable binding site for WRN. Finally, the 3′→5′ exonuclease activity of WRN recognizes the 3′ end of the invading strand of the D-loop and digests it efficiently, distributively, and independently of ATP binding, ATP hydrolysis, and DNA unwinding. Intriguingly, this 3′ end, near the forked region at the proximal side of the 24 bp arm (see Figure 1A), is very accessible to WRN's exonuclease domain. Taken together, our assays suggest that WRN may be spatially oriented on this D-loop substrate with its exonuclease domain positioned at the 3′ end of the invading strand and the helicase domain at the junction where the invading strand exits the duplex. Although here we examined WRN helicase and exonuclease activities separately for ease of interpretation, their combined action might be expected to further enhance disruption of D-loops and similar structures. However, it is also possible that either helicase or exonuclease activity may predominate in specific situations.

These results are consistent with the notion that D-loop structures might be particularly susceptible to the catalytic activities of WRN in vivo. Strand invasion and D-loop formation is an early step in recombination pathways, and many recombinational D-loops are believed to be formed by invasion of 3′ single-stranded overhangs into homologous duplex DNA (*14*, *15*). In such a structure, the 3′ end within the D-loop may also serve as a primer for DNA polymerases. The ability of WRN to disrupt and degrade D-loops may indicate a function in recombination or anti-recombination pathways. By way of its unwinding and/or exonuclease activities, WRN could serve to reverse D-loop formation and inhibit recombination. Conversely, once a recombination intermediate is formed, the helicase activity of WRN may facilitate Holliday structure branch migration as reported previously (*19*). Defects in WRN and other RecQ helicases result in illegitimate and hyper-recombination phenotypes (*1*, *2*, *8*), consistent with possible roles of these proteins in suppressing recombination, perhaps through disruption of D-loop intermediates. In this regard, BLM, the human RecQ member deficient in Bloom syndrome, also binds and disrupts D-loop structures (*20*).

Recent studies have indicated that D-loop structures occur in telomeric regions (*21*, *22*), potentially serving either to sequester and protect the linear ends of chromosomes (*23*) or to facilitate telomere elongation by the ALT (alternative lengthening of telomeres) recombinational pathway (*24*). Accelerated telomere shortening is also a key part of the genomic instability phenotype of WS, suggesting a role for WRN in telomere metabolism (*5*, *6*). In support of this notion, WRN interacts functionally and physically with Ku (*25*), a heterodimeric complex that is, in part, associated with telomeres (*26*). WRN also colocalizes with telomeric factors in cells utilizing the ALT pathway (*27*), suggesting a specific role for WRN in telomere lengthening by recombination. As mentioned above, the WRN branch migrates Holliday junctions and may also facilitate recombination by unwinding unusual structures formed by repetitive telomeric sequences prior to or during strand exchange and branch migration steps. In this regard, WRN unwinds branched and G-quartet structures constructed from DNA containing telomeric repeats (*28*, *29*). We speculate that the accelerated loss of telomeric sequences in WRN-deficient cells may be due to an inability to process telomeric D-loop or other related structures. Thus, the complete genomic instability phenotype observed in WS may be related to the inability to process D-loops formed during telomere metabolism and/or recombination, although further investigation is needed to support this hypothesis.

## ACKNOWLEDGMENT

The authors thank Liren Xiao for expert technical assistance and Dr. Zhigang Wang for critical reading of the manuscript.

## REFERENCES

1. Oshima, J. (2000) The Werner syndrome protein: an update, *BioEssays 22*, 894−901.
2. Furuichi, Y. (2001) Premature aging and predisposition to cancers caused by mutations in RecQ family helicases, *Ann. N.Y. Acad. Sci. 928*, 121−131.
3. Fukuchi, K., Martin, G. M., and Monnat, R. J. (1989) Mutator phenotype of Werner syndrome is characterized by extensive deletions, *Proc. Natl. Acad. Sci. U.S.A. 86*, 5893−5897.
4. Stefanini, M., Scappaticci, S., Lagomarsini, P., Borroni, G., Berardesca, E., and Nuzzo, F. (1989) Chromosome instability in lymphocytes from a patient with Werner's syndrome is not associated with DNA repair defects, *Mutat. Res. 219*, 179−185.
5. Schulz, V. P., Zakian, V. A., Ogburn, C. E., McKay, J., Jarzebowicz, A. A., Edland, S. D., and Martin, G. M. (1996) Accelerated loss of telomeric repeats may not explain accelerated replicative decline of Werner syndrome cells, *Hum. Genet. 97*, 750−754.
6. Tahara, H., Tokutake, Y., Maeda, S., Kataoka, H., Watanabe, T., Satoh, M., Matsumoto, T., Sugawara, M., Ide, T., Goto, M., Furuichi, Y., and Sugimoto, M. (1997) Abnormal telomere dynamics of B-lymphoblastoid cell strains from Werner's syndrome patients transformed by Epstein−Barr virus, *Oncogene 15*, 1911−1920.
7. Yu, C. E., Oshima, J., Fu, Y. H., Hisama, F., Wijsman, E. M., Alisch, R., Matthews, S., Nakura, J., Miki, T., Ouais, S., Martin, G. M., Mulligan, J., and Schellenberg, G. D. (1996) Positional cloning of the Werner 's syndrome gene, *Science 272*, 258−262.

8. Karow, J. K., Wu, L., and Hickson, I. D. (2000) RecQ family helicases: roles in cancer and aging, *Curr. Opin. Genet. Dev. 10*, 32−38.
9. Shen, J. C., Gray, M. D., Oshima, J., and Loeb, L. A. (1998) Characterization of Werner syndrome protein DNA helicase activity: directionality, substrate dependence, and stimulation by replication protein A, *Nucleic Acids Res. 26*, 2879−2885.
10. Brosh, R. M., Jr., Orren, D. K., Nehlin, J. O., Ravn, P. H., Kenny, M. K., Machwe, A., and Bohr, V. A. (1999) Functional and physical interaction between WRN helicase and human replication protein A, *J. Biol. Chem. 274*, 18341−18350.
11. Brosh, R. M., Waheed, J., and Sommers, J. A. (2002) Biochemical characterization of the DNA substrate specificity of Werner syndrome helicase, *J. Biol. Chem. 277*, 23236−23245.
12. Huang, S., Li, B., Gray, M. D., Oshima, J., Mian, I. S., and Campisi, J. (1998) The premature aging syndrome protein, WRN, is a 3′→5′ exonuclease, *Nat. Genet. 20*, 114−116.
13. Shen, J. C., Gray, M. D., Oshima, J., Kamath-Loeb, A. S., Fry, M., and Loeb, L. A. (1998) Werner syndrome protein. I. DNA helicase and exonuclease reside on the same polypeptide, *J. Biol. Chem. 273*, 34145−34150.
14. Haber, J. E. (1999) DNA recombination: the replication connection, *Trends Biochem. Sci. 24*, 271−275.
15. Kowalczykowski, S. C. (2000) Initiation of genetic recombination and recombination-dependent replication, *Trends Biochem. Sci. 25*, 156−165.
16. Orren, D. K., Brosh, R. M., Nehlin, J. O., Machwe, A., Gray, M. D., and Bohr, V. A. (1999) Enzymatic and DNA binding properties of purified WRN protein: high affinity binding to single-stranded DNA but not to DNA damage induced by 4NQO, *Nucleic Acids Res. 27*, 3557−3566.
17. Machwe, A., Xiao, L., Theodore, S., and Orren, D. K. (2002) DNase I footprinting and enhanced exonuclease function of the bipartite Werner syndrome protein (WRN) bound to partially melted duplex DNA, *J. Biol. Chem. 277*, 4492−4504.
18. Shen, J. C., and Loeb, L. A. (2000) Werner syndrome exonuclease catalyzes structure-dependent degradation of DNA, *Nucleic Acids Res. 28*, 3260−3268.
19. Constantinou, A., Tarsounas, M., Karow, J. K., Brosh, R. M., Bohr, V. A., Hickson, I. D., and West, S. C. (2000) Werner's syndrome protein (WRN) migrates Holliday junctions and co-localizes with RPA upon replication arrest, *EMBO Rep. 1*, 80−84.
20. Van Brabant, A. J., Ye, T., Sanz, M., German, J. L., Ellis, N. A., and Holloman, W. K. (2000) Binding and melting of D-loops by the Bloom syndrome helicase, *Biochemistry 39*, 14617−14625.
21. Griffith, J. D., Comeau, L., Rosenfield, S., Stansel, R. M., Bianchi, A., Moss, H., and de Lange, T. (1999) Mammalian telomeres end in a large duplex loop, *Cell 97*, 503−514.
22. Murti, K. G., and Prescott, D. M. (1999) Telomeres of polytene chromosomes in a ciliated protozoan terminate in duplex DNA loops, *Proc. Natl. Acad. Sci. U.S.A. 96*, 14436−14439.
23. de Lange, T. (2002) Protection of mammalian telomeres, *Oncogene 21*, 532−540.
24. Lundblad, V. (2002) Telomere maintenance without telomerase, *Oncogene 21*, 522−531.
25. Cooper, M. C., Machwe, A., Orren, D. K., Brosh, R. M., Ramsden, D., and Bohr, V. A. (2000) Ku complex interacts with and stimulates the Werner protein, *Genes Dev. 14*, 907−912.
26. Hsu, H. L., Gilley, D., Blackburn, E. H., and Chen, D. J. (1999) Ku is associated with the telomere in mammals, *Proc. Natl. Acad. Sci. U.S.A. 96*, 12454−12458.
27. Johnson, F. B., Marciniak, R. A., McVey, M., Stewart, S. A., Hahn, W. C. and Guarente, L. (2001) The *Saccharomyces cerevisiae* WRN homologue Sgs1p participates in telomere maintenance in cells lacking telomerase, *EMBO J. 20*, 905−913.
28. Ohsugi, I., Tokutake, Y., Suzuki, N., Ide, T., Sugimoto, M., and Furuichi, Y. (2000) Telomere repeat DNA forms a large noncovalent complex with unique cohesive properties which is dissociated by Werner syndrome DNA helicase in the presence of replication protein A, *Nucleic Acids Res. 28*, 3642−3648.
29. Mohaghegh, P., Karow, J. K., Brosh, R. M., Bohr, V. A., and Hickson, I. D. (2001) The Bloom's and Werner's syndrome proteins are DNA structure-specific helicases, *Nucleic Acids Res. 29*, 2843−2849.

BI0266986